

Supporting Information for:

Optimizing the Grafting Density of Tethered Chains to Alter the Local Glass Transition Temperature of Polystyrene near Silica Substrates: The Advantage of Mushrooms over Brushes

Xinru Huang and Connie B. Roth*

Department of Physics, Emory University, Atlanta, Georgia 30322, USA

* To whom correspondence should be addressed. cbroth@emory.edu

ACS Macro Letters 2018

Sample Preparation and Measurement Details

Following procedures previously established in the literature,¹⁻³ monocarboxy-terminated polystyrene (PS-COOH) ($M_w = 101.8$ kg/mol, $M_w/M_n = 1.03$, Scientific Polymer Products) was end-grafted to silicon wafers or silica substrates by spin-coating PS-COOH films from toluene and annealing them under vacuum at 170 °C for 1.5 h. The grafting process should be the same for these two types of substrates as their surfaces are both terminated with SiO_x. Prior to grafting, the substrates were cleaned in ~10 vol% hydrochloric acid for 20 s to remove any impurities. After annealing, samples were bathed in 90 °C toluene for 20 min to wash off ungrafted chains, and subsequently rinsed with acetone and DI water, while being blown dry with nitrogen gas after each step. A final drying step was done by placing the grafted substrates in the vacuum oven overnight at room temperature. Samples with different grafting densities were produced by decreasing the initial film thickness of the spin-coated PS-COOH films and mixing with neat polystyrene (PS) ($M_w = 101.3$ kg/mol, $M_w/M_n = 1.04$, Scientific Polymer Products). The final dry-brush thickness h_{brush} was measured by ellipsometry (Woollam M-2000) for those samples made on silicon wafers. There is insufficient contrast in the index of refraction between PS and silica to accurately measure such thin films directly on the silica substrates used for fluorescence. Ellipsometer data fitting was done using a standard layer model with the PS film treated as a Cauchy layer $n(\lambda) = A + B/\lambda^2 + C/\lambda^4$, and the underlying silicon wafer having a 1.25 nm native oxide layer. Following our previous work, such thin films were fit to the PS film thickness, A and B , while holding the Cauchy parameter C fixed at the bulk value 0.00038.⁴ The grafting density σ was calculated using $\sigma = \frac{\rho N_A h_{\text{brush}}}{M_n}$,⁵ where the number average molecular weight $M_n = 98.8$ kg/mol for the PS-COOH, and the density $\rho = 1.045$ g/cm³ was taken as the

bulk value for PS.⁶ Measured dry brush thicknesses h_{brush} varied from 0.7 to 6.6 nm giving grafting densities σ from 0.004 to 0.042 chains/nm² ($\Sigma = 1.0$ to 10).

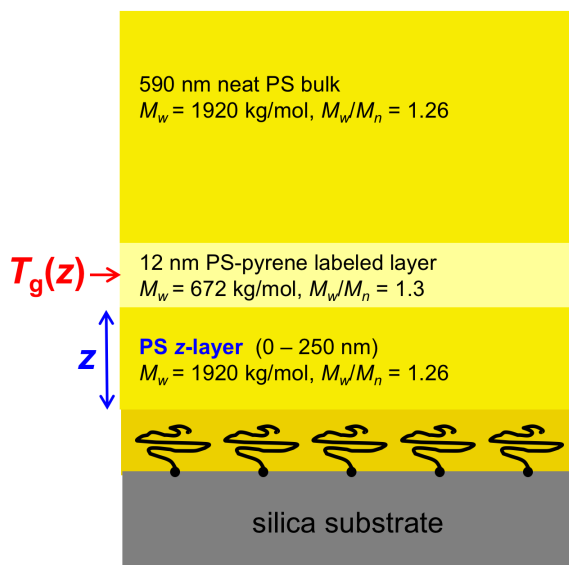


Figure S1. Schematic of multilayer sample geometry assembled for fluorescence measurements of the localized glass transition temperature $T_g(z)$ as a function of distance z from end-tethered substrates.

Neat PS ($M_w = 1920 \text{ kg/mol}$, $M_w/M_n = 1.26$, Pressure Chemical) of variable thickness $z = 0$ to 250 nm, and bulk $590 \pm 5 \text{ nm}$ thick, or $12 \pm 1 \text{ nm}$ thick pyrene-labeled PS ($M_w = 672 \text{ kg/mol}$, $M_w/M_n = 1.3$, with 1.4 mol% pyrene^{7,8}) films were spin-coated from toluene onto freshly-cleaved mica. All such layers were independently annealed overnight at $120 \text{ }^\circ\text{C}$ under vacuum prior to floating. Multilayer sample structures, as depicted in Figure S1, were assembled by first floating the neat PS layer of desired thickness z atop the PS-COOH end-grafted silica substrates. This bilayer was then annealed under vacuum at $170 \text{ }^\circ\text{C}$ for 2 h to ensure good interpenetration of the tethered chains with the neighboring PS matrix. O'Connor and McLeish⁹ argued that for relatively low grafting densities, isolated tethered chains can rapidly penetrate into high molecular weight matrices (or even cross-linked elastomers) via Rouse mode and “breathing” mode (chain-end) relaxations. This was experimentally confirmed by Clarke¹⁰ using neutron reflectivity to measure the interpenetration of deuterated PS-COOH ($M_w = 79.8 \text{ kg/mol}$, $M_w/M_n = 1.04$) end-tethered chains into matrices of high molecular weight protonated PS of $M_w = 500.8 \text{ kg/mol}$ ($M_w/M_n = 1.06$) or $M_w = 8,000 \text{ kg/mol}$ ($M_w/M_n < 1.07$). For grafting densities of

$\sigma = 0.074$ chains/nm², even 15 min of annealing at 150 °C was sufficient to obtain a depth profile for the dPS-COOH chains that did not change substantially with further annealing up to 23 h. After this initial annealing step of the bilayer structure, the 12-nm pyrene-labeled PS layer and neat bulk PS layer were subsequently floated on, allowing the sample to thoroughly dry between each successive floating step.

Fluorescence measurements were carried out using a Photon Technology International QuantaMaster spectrofluorometer with samples mounted in an Instec HCS402 heater. Samples were heated from room temperature to 170 °C and equilibrated for 20 min. This allows the assembled multilayer samples to form a consolidated material with sufficient interdiffusion at the floated interfaces to remove any air gaps. The pyrene fluorescence emission is then monitored on cooling at 1 °C/min for 3 s every 27 s at an emission wavelength of 379 nm, while exciting at 330 nm (with band passes kept between 5-6 nm). All samples were reheated to the starting temperature after each run to ensure that the same initial fluorescence intensity was recovered, verifying that the sample had remained stable during the course of the experiment and no photobleaching occurred. The local $T_g(z)$ is then determined from the temperature-dependent fluorescence intensity by fitting straight lines to the slope of the intensity data above and below the transition to identify the intersection of the two fits. Data collected on multiple samples allows us to determine the local $T_g(z = 0)$ value next to the substrate for different grafting densities, as well as the $T_g(z)$ profile as a function of distance from the substrate. Figure S2 plots such temperature-dependent fluorescence intensity data for three different samples all with the same grafting density of $\sigma = 0.042$ chains/nm², where the thickness of the z -layer spacer was varied to determine the local $T_g(z)$ value at different distances from the substrate: $T_g(z = 0) = 144 \pm 2$ °C, $T_g(z = 32 \text{ nm}) = 115 \pm 2$ °C, and $T_g(z = 222 \text{ nm}) = 100 \pm 2$ °C. Figure S3 shows the $T_g(z)$ profile for $\sigma = 0.042$ chains/nm² constructed from measurements on multiple samples. To accommodate the dry-brush thickness $h_{\text{brush}} = 6.6$ nm for $\sigma = 0.042$ chains/nm², the distance from the grafted substrate (x -axis of Fig. S3) was taken to be equal to the thickness of the z spacer layer plus 6.6 nm.

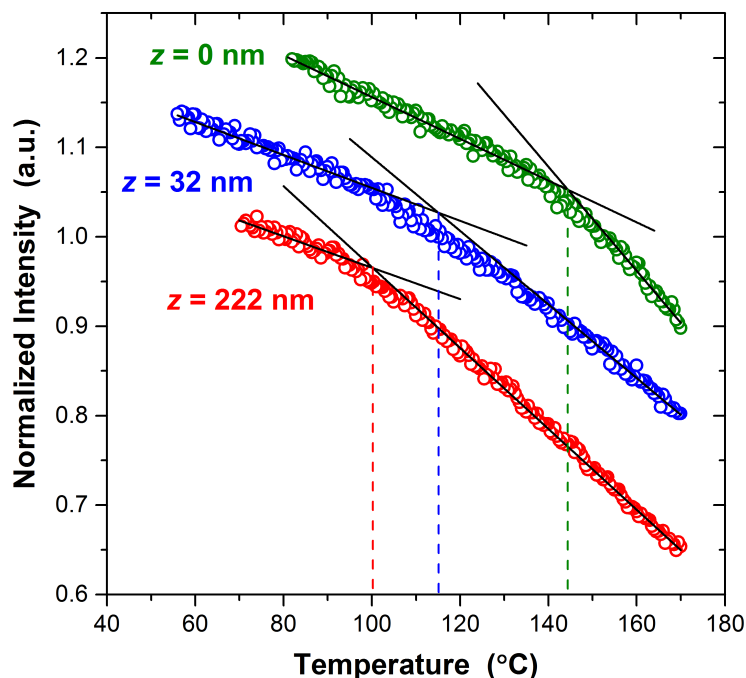


Figure S2. Fluorescence intensity versus temperature measured on cooling at 1 °C/min for three samples with a grafting density of $\sigma = 0.042$ chains/nm², where the pyrene-labeled layer was placed at different distances $z = 0, 32,$ and 222 nm.

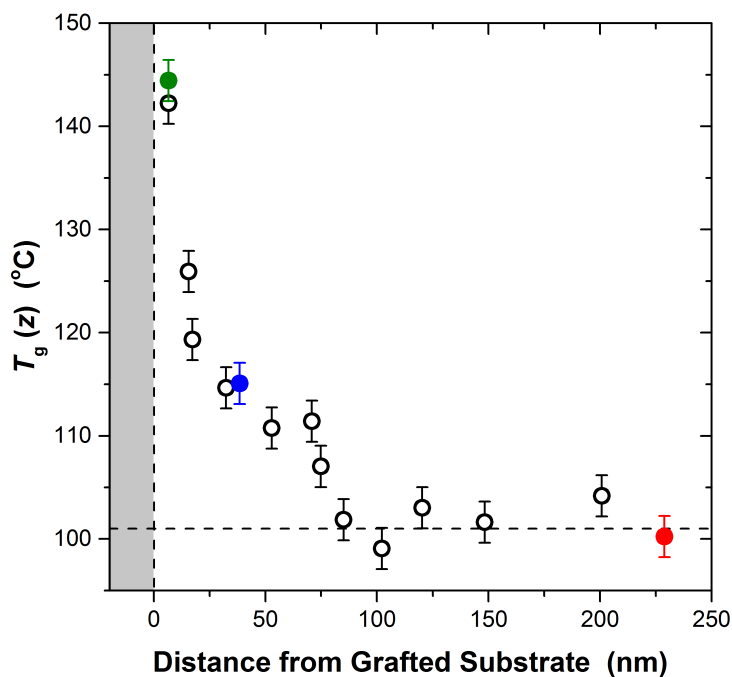


Figure S3. Local $T_g(z)$ profile measured for end-tethered substrates with a grafting density of $\sigma = 0.042$ chains/nm². The distance from the substrate (x -axis) was taken to be $z + 6.6$ nm to accommodate the thickness of the dry brush. The three colored data points correspond to the datasets shown in Figure S2.

One of the keys to making these localized fluorescence measurements is the use of high molecular weight polymers to limit the diffusion of the pyrene-labeled probe layer during the course of the measurement. Sufficient annealing needs to be done initially to weld the various interfaces of the assembled layers together to create a single consolidated material without any air gaps. This occurs quickly via Rouse modes with interfacial widths of a few nanometers easily formed after a few minutes; further diffusion and growth of the interface is then limited by the reptation time.¹¹⁻¹³ Typically, the amount of time necessary to collect data at elevated temperatures above T_g is sufficiently small such that simply the use of high molecular weight polymers adequately limits the diffusion of the thin pyrene-labeled layer away from its localized position.^{7,8,14} However, for the present study, we measured elevated local $T_g(z)$ values around 140-150 °C, necessitating data collection far enough above the transition to accurately identify the slope of the liquid regime. Given the strong temperature dependence of polymer reptation times, we decided to lightly crosslink the pyrene-labeled PS layer to further ensure that it would remain localized even at these elevated temperatures. Very few crosslinks would be necessary to arrest diffusion, which can be accomplished at a level of crosslink density much less than the entanglement density, and as such have no impact on the glass transition of the material.

The use of ultra-violet (UV) light to crosslink polystyrene has been employed frequently in the literature. Commonly a UV-ozone treatment is done that utilizes two UV wavelengths, 185 nm that dissociates molecular oxygen leading to the generation of ozone and 254 nm that is absorbed directly by the phenyl ring of PS.^{15,16} The oxygen reaction with the phenyl rings of PS occurs rapidly (<5 min) resulting in the formation of a more polar surface containing carbonyl and carboxyl species, but its effects are generally limited to the near surface region (≈ 5 nm) because of the limited ability of oxygen to penetrate into the film.¹⁵⁻¹⁷ In contrast, crosslinking by only the 254 nm UV light is a much slower process that can take several hours and penetrates much deeper into the film (~ 1 μm).¹⁷⁻¹⁹ To minimize chemical changes, we use only the 254 nm UV wavelength for a time and intensity that enacts a minimum of crosslinks. Solvent swelling tests were used to confirm that the 254 nm UV exposure did lead to a crosslinked film, while several control measurements described below were carried out with fluorescence to ensure that the UV exposure did not harm the pyrene dye and affect the accuracy of the T_g fluorescence measurement. The 254 nm wavelength is close the absorption maximum for the phenyl ring of

PS,¹⁵ while pyrene primarily absorbs at longer wavelengths because of its larger resonance structure. Thus, predominantly only a handful of PS phenyl rings are being affected by this UV process.

During the sample preparation described above, the 12-nm pyrene-labeled layer was lightly crosslinked by exposing it to a UV lamp (UVP compact UV lamp, model UVG-11) with a 254 nm wavelength prior to floating off the mica surface. A UV exposure of 10 min with the lamp located at a distance of 16 mm from the film's surface was found to be sufficient to prevent diffusion and stabilize the pyrene-labeled PS layer to extended annealing times at 170 °C. The pyrene fluorescence emission spectrum is generally unaffected by this UV treatment. There is some photobleaching that occurs indicating loss of some dye, but this does not impact the fluorescence measurement of the glass transition provided that no further photobleaching occurs during the course of the measurement, something which is verified after each measurement. We now describe the various tests we conducted to ensure that this UV treatment to lightly crosslink the pyrene-labeled layer does not affect the measured glass transition by fluorescence.

We verified that the 10 min of UV exposure at 254 nm does not alter the ability of the pyrene-labeled PS layer to measure the glass transition by directly comparing measurements on identical samples with and without this added crosslinking step of the pyrene-labeled probe layer. Following the work of Ellison and Torkelson,¹⁴ we constructed samples with a 24 ± 2 nm thick pyrene-labeled PS layer atop a bulk, 270 ± 5 nm underlayer. The local T_g was measured by heating the samples to 130 °C, equilibrating for 20 min, and then measuring the fluorescence intensity on cooling at 1 °C/min as described above. Figure S4 shows the temperature-dependent intensity curves for two samples, one where the pyrene-labeled layer was lightly crosslinked with 10 min of UV light exposure at 254 nm and another where the sample was traditionally made with no crosslinking. Both samples report at local T_g for the 24 nm thick PS free surface layer of 80 ± 2 °C. Repeated measurements on multiple nominally identical samples give, for the average and standard deviation of four separate measurements each: 82.5 ± 3.6 °C for the UV crosslinked and 82.5 ± 4.0 °C for the traditionally made samples. These values are in reasonably good agreement with those measured by Ellison and Torkelson¹⁴ on similar multilayer samples.

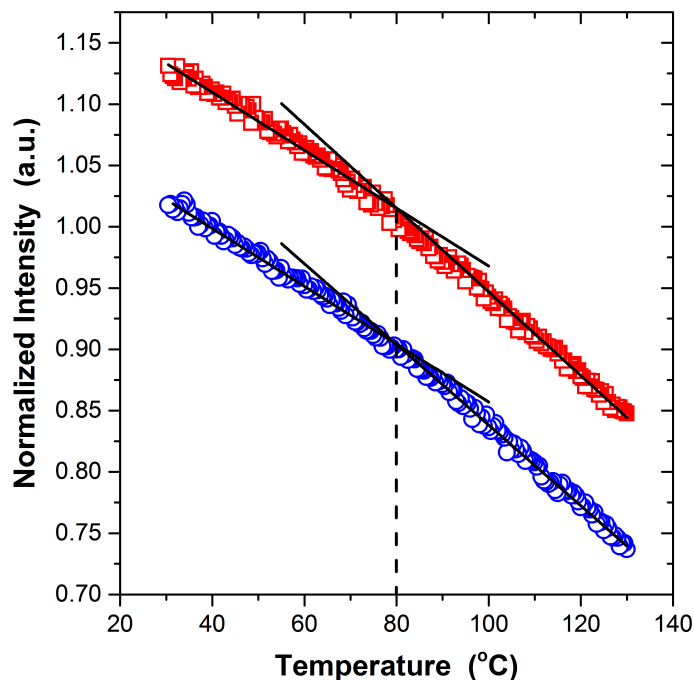


Figure S4. Temperature-dependent fluorescence intensity data for a 24 nm thick pyrene-labeled PS free surface layer atop a 270 nm bulk PS underlayer for a sample where the pyrene-labeled probe layer had been lightly crosslinked using UV light (blue circles) and a traditionally made sample without UV crosslinking (red squares). Data have been vertically offset for clarity.

To ensure that this additional crosslinking step adequately limits diffusion of the pyrene-labeled probe layer even with extended annealing at elevated temperatures, we used a series of samples with a 24 ± 2 nm thick pyrene-labeled PS layer atop a bulk, 270 ± 5 nm underlayer to measure the local T_g value of this free surface layer as a function of annealing time at 170 °C. Figure S5 shows that for the samples whose pyrene-labeled layer had been lightly crosslinked with 10 min of UV light at 254 nm, the measured local T_g value is stable to annealing at 170 °C for up to 18 h, while the traditionally made samples without crosslinking eventually show the measured T_g value increasing from the initial locally reduced T_g value of the free surface layer to a value closer to that of bulk PS as the 24-nm thick pyrene-labeled PS layer at the free surface diffuses throughout the bulk PS film. Thus, we can conclude that the light crosslinking of the pyrene-labeled layer by UV light does not affect the measured T_g value and we do not need to be concerned with the diffusion of the labeled layer during the course of our experiments where the sample spends ~ 1 h at temperatures between 130-170 °C.

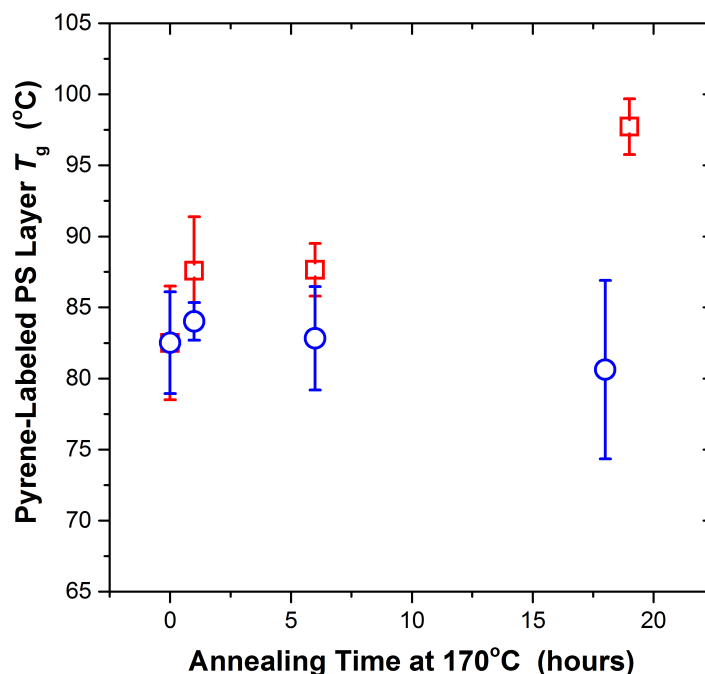


Figure S5. Local T_g measured for a 24 nm thick PS free surface layer as a function of annealing time at 170 °C under vacuum for samples with (blue circles) and without (red squares) 10 min of UV treatment at 254 nm wavelength to lightly crosslink the pyrene-labeled PS layer. Each data point represents the average and standard deviation from measurements on four different nominally identical samples.

References

- (1) Keddie, J. L.; Jones, R. A. L. Glass Transition Behavior in Ultra-Thin Polystyrene Films. *Israel J Chem* **1995**, *35*, 21–26.
- (2) Tate, R. S.; Fryer, D. S.; Pasqualini, S.; Montague, M. F.; de Pablo, J. J.; Nealey, P. F. Extraordinary Elevation of the Glass Transition Temperature of Thin Polymer Films Grafted to Silicon Oxide Substrates. *J Chem Phys* **2001**, *115*, 9982–9990.
- (3) Clough, A.; Peng, D.; Yang, Z.; Tsui, O. K. C. Glass Transition Temperature of Polymer Films That Slip. *Macromolecules* **2011**, *44*, 1649–1653.
- (4) Huang, X.; Roth, C. B. Changes in the Temperature-Dependent Specific Volume of Supported Polystyrene Films with Film Thickness. *J Chem Phys* **2016**, *144*, 234903.
- (5) Brittain, W. J.; Minko, S. A Structural Definition of Polymer Brushes. *J Polym Sci, Part A: Polym Chem* **2007**, *45*, 3505–3512.
- (6) Orwoll, R. A. Densities, Coefficients of Thermal Expansion, and Compressibilities of Amorphous Polymers. In *Physical Properties of Polymers Handbook*; Mark, J. E., Ed.; Springer: New York, 2007; pp. 93–101.
- (7) Baglay, R. R.; Roth, C. B. Communication: Experimentally Determined Profile of Local Glass Transition Temperature Across a Glassy-Rubbery Polymer Interface with a T_g

- Difference of 80 K. *J Chem Phys* **2015**, *143*, 111101.
- (8) Baglay, R. R.; Roth, C. B. Local Glass Transition Temperature $T_g(Z)$ of Polystyrene Next to Different Polymers: Hard vs. Soft Confinement. *J Chem Phys* **2017**, *146*, 203307.
 - (9) O'Connor, K. P.; McLeish, T. C. B. "Molecular Velcro": Dynamics of a Constrained Chain Into an Elastomer Network. *Macromolecules* **1993**, *26*, 7322–7325.
 - (10) Clarke, C. J. The Kinetics of Polymer Brush Penetration into a High Molecular Weight Matrix. *Polymer* **1996**, *37*, 4747–4752.
 - (11) Jones, R. A. L.; Richards, R. W. *Polymers at Surfaces and Interfaces*; Cambridge University Press, 1999.
 - (12) Karim, A.; Mansour, A.; Felcher, G. P.; Russell, T. P. Short-Time Relaxation at Polymeric Interfaces. *Phys Rev B* **1990**, *42*, 6846–6849.
 - (13) Stamm, M.; Huttenbach, S.; Reiter, G.; Springer, T. Initial Stages of Polymer Interdiffusion Studied by Neutron Reflectometry. *Europhys Lett* **1991**, *14*, 451–456.
 - (14) Ellison, C. J.; Torkelson, J. M. The Distribution of Glass-Transition Temperatures in Nanoscopically Confined Glass Formers. *Nature Materials* **2003**, *2*, 695–700.
 - (15) Klein, R. J.; Fischer, D. A.; Lenhart, J. L. Systematic Oxidation of Polystyrene by Ultraviolet-Ozone, Characterized by Near-Edge X-Ray Absorption Fine Structure and Contact Angle. *Langmuir* **2008**, *24*, 8187–8197.
 - (16) Efimenko, K.; Wallace, W. E.; Genzer, J. Surface Modification of Sylgard-184 Poly(Dimethyl Siloxane) Networks by Ultraviolet and Ultraviolet/Ozone Treatment. *J Colloid Interf Sci* **2002**, *254*, 306–315.
 - (17) Zhang, D.; Dougal, S. M.; Yeganeh, M. S. Effects of UV Irradiation and Plasma Treatment on a Polystyrene Surface Studied by IR-Visible Sum Frequency Generation Spectroscopy. *Langmuir* **2000**, *16*, 4528–4532.
 - (18) Otocka, E. P.; Curran, S.; Porter, R. S. Photooxidation of Polystyrene: Irradiation at 254 and 365 Nm. *J Appl Polym Sci* **1983**, *28*, 3227–3233.
 - (19) Zhang, R.; Cherdhirankorn, T.; Graf, K.; Koynov, K.; Berger, R. Swelling of Cross-Linked Polystyrene Beads in Toluene. *Microelectron Eng* **2008**, *85*, 1261–1264.